Absorption of CO_2 and CS_2 into the Hofmann-Type Porous Coordination Polymer: Electrostatic versus Dispersion Interactions

Milind Madhusudan Deshmukh,[†] Masaaki Ohba,[‡] Susumu Kitagawa,[§] and Shigeyoshi Sakaki*,[†]

[†]Fukui Institute for Fundamental Chemistry, Kyoto University, Nishihiraki-cho, Sakyo-ku, Takano, Kyoto 606-8103, Japan

[‡]Department of Chemistry, Faculty of Sciences, Kyushu University, Hakozaki, Higashi-ku, Fukuoka 812-8581, Japan

[§]Department of Synthetic Chemistry and Biological Chemistry, Graduate School of Engineering, Kyoto University, Nishikyo-ku, Kyoto 615-8510, Japan

ⓢ *Supporting Information*

ABSTRACT: Absorption of CO_2 and CS_2 molecules into the Hofmann-type three-dimensional porous coordination polymer (PCP) $\{Fe(Pz)[Pt(CN)_4]\}_n$ (Pz = pyrazine) was theoretically explored with the ONIOM(MP2.5 or SCS-MP2:DFT) method, where the M06-2X functional was employed in the DFT calculations. The binding energies of CS_2 and CO_2 were evaluated to be −17.3 and −5.2 kcal mol^{-1}, respectively, at the ONIOM(MP2.5:M06-2X) level and −16.9 and −4.4 kcal mol^{-1} at the ONIOM(SCS-MP2:M06-2X) level. It is concluded that CS_2 is strongly absorbed in this PCP but CO_2 is only weakly absorbed. The absorption positions of these two molecules are completely different: CO_2 is located between two Pt atoms, whereas one S atom of CS_2 is located

Binding Energy = -5.2 kcal mol⁻¹   Binding Energy=-17.3 kcal mol⁻¹

between two Pz ligands and the other S atom is between two Pt atoms. The optimized position of CS_2 agrees with the experimentally reported X-ray structure. To elucidate the reasons for these differences, we performed an energy decomposition analysis and found that (i) both the large binding energy and the absorption position of CS_2 arise from a large dispersion interaction between CS_2 and the PCP, (ii) the absorption position of CO_2 is mainly determined by the electrostatic interaction between CO_2 and the Pt moiety, and (iii) the small binding energy of CO_2 comes from the weak dispersion interaction between CO_2 and the PCP. Important molecular properties relating to the dispersion and electrostatic interactions, which are useful for understanding and predicting gas absorption into PCPs, are discussed in detail.
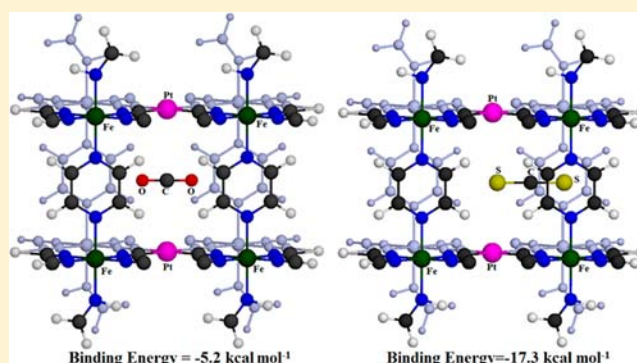
■ INTRODUCTION

Porous coordination polymers (PCPs) or metal−organic frameworks (MOFs) have recently attracted a great amount of attention because of their potential applications in gas storage,[1,2] gas separation,[2,3] catalysis,[4] and nanospace engineering.[5] The flexibility in the use of a variety of organic linkers and/or metals leads to syntheses of many kinds of PCPs with required properties. Among the desired properties, selective uptake[6] and storage[1,2] of gas molecules have been well-investigated. Also, the optical and magnetic properties of PCPs and their responses to the inclusion of guest molecules have recently started to draw new attention[7−10] because the response of structure and/or properties of PCPs to external perturbations provide robust new possibilities for functional materials that would be useful in switches, sensors, and information transduction.[11,12] The spin transition is one of the most interesting molecular properties of a molecule-based switchable material. This phenomenon is often observed in 3d⁴ to 3d⁷ metal compounds.[13] In particular, it is well-known that iron(II) compounds with a 3d⁶ electron configuration can change between paramagnetic high-spin and diamagnetic low-spin states with thermal hysteresis and that some of them

provide bistabilities in magnetic, optical, and structural properties.[14,15] Though the spin transition is induced by temperature or photoirradiation in many cases, chemo-responsive switching of the spin state by gas absorption was recently reported in the Hofmann-type three-dimensional PCP $\{Fe^{II}(Pz)[Pt^{II}(CN)_4]\}_n$ (Pz = pyrazine).[9] For instance, the absorption of molecules that are bulky (e.g., benzene, toluene, thiophene) or can form clusters in PCPs (e.g., water, methanol) stabilizes a high-spin state. Of particular interest is the absorption of carbon disulfide, as CS_2 absorption induces the spin transition from the high-spin state to the low-spin state, which is the reverse of the spin transition induced by bulky molecules. On the other hand, the absorption of the similar molecule CO_2 does not induce any spin transition.[9] In a recent theoretical study employing a simple model system,[9b] the reason for the spin transition caused by CS_2 was preliminarily discussed in terms of the entropy decrease induced by CS_2 absorption. The key point is that CS_2 occupies a position intermediate between two Pz rings and decreases the entropy

Scheme 1. Crystal Structure of the Hofmann-Type PCP $\{Fe^{II}(Pz)[Pt^{II}(CN)_4]\}_n$ with Absorbed CS_2 (Fe, Green; Pt, Pink; C, Gray; N, Blue; S, Yellow)
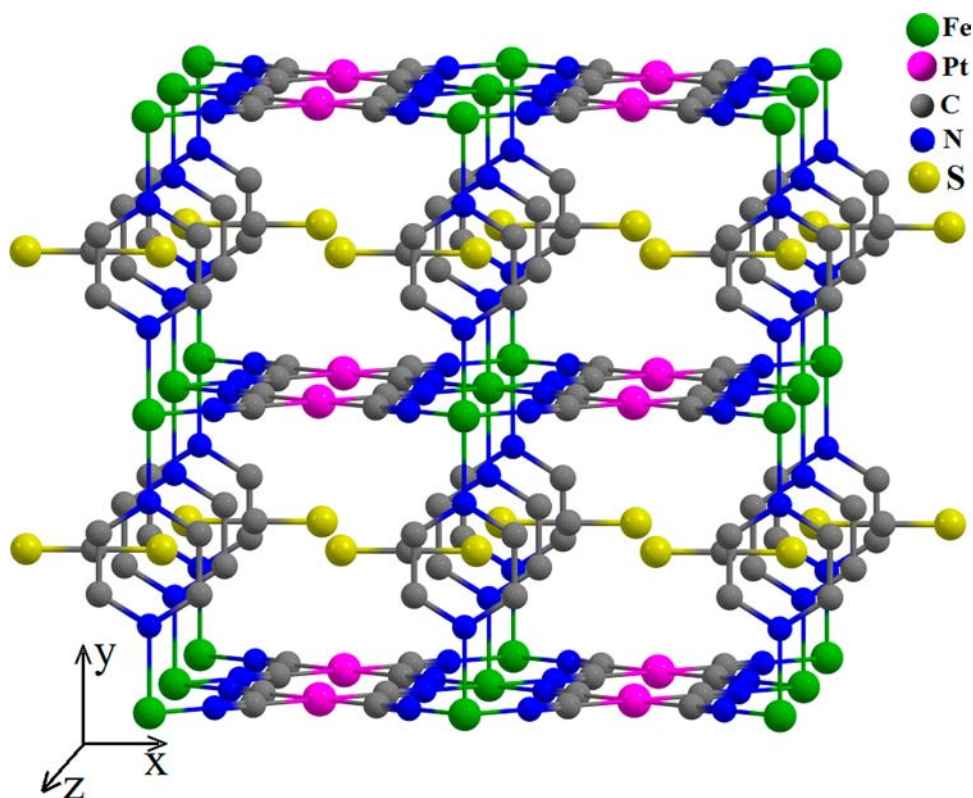

by suppressing the rotational movement of these Pz rings.[9b] This result suggests that such a spin transition should not occur if the gas molecule takes a position distant from the Pz ring or if the binding energy of the gas molecule with the PCP is not large enough to suppress the rotation of the Pz rings. In this regard, the absorption position and absorption energy of gas molecules with the PCP are of considerable importance for understanding and predicting the spin transitions of this PCP.

Several ab initio computational studies of the interaction of gas molecules such as H_2, CO_2, and CH_4 with PCP frameworks have been reported.[16−20,22−24] Sagara and co-workers[16] investigated the interaction of H_2 with MOF-5 using second-order Møller−Plesset perturbation theory (MP2) and reported that the binding energy is about −6 to −7 kJ mol^{-1} at the metal site and about −4 to −5 kJ mol^{-1} at the organic linker site. Another study using density functional theory (DFT) reported that the interaction of H_2 with a model system (benzene) is significantly different from the interaction with actual MOF-5.[17] The interactions of CO_2 with model organic linkers were also theoretically investigated using MP2, DFT, and CCSD(T) methods, including the basis set extension effect calculated with the MP2/F12 method,[18−20] where alcohols, ketones, esters, amines, and several N-containing heterocycles were employed as models of the organic linker.[20] The DFT-D method, which uses the empirical dispersion correction proposed by Grimme,[21] provided a CO_2 binding energy comparable to the CCSD(T)-calculated value,[20] suggesting that the DFT-D method is useful in evaluating the binding energy of a gas molecule with an organic linker. In these theoretical studies[18−20] and similar works,[22−24] however, model systems consisting of either a metal or organic site were employed. In other words, models consisting of both a metal and an organic

linker were not employed. This means that the cooperative functions of the metal and linker were not considered at all.

The use of a realistic model including both a metal and an organic linker has been limited to date. Pianwanit and co-workers[25] theoretically investigated a more realistic model including both metal and organic moieties using the ONIOM-(MP2:Hartree−Fock) method and concluded that both CO_2 and CH_4 occupy the position perpendicular to the ZnO_4 corner of MOF-5 with binding energies of −9.27 and −3.64 kcal mol^{-1}, respectively (throughout this work, a negative binding energy represents energy stabilization as a result of the interaction of the gas molecule with the PCP). In another recent study using the DFT method, Grajciar et al.[26] investigated CO_2 adsorption to the PCP $[Cu_3(BTC)_2(H_2O)_3]_n$ (BTC = benzene-1,3,5-tricarboxylate) bearing one open metal site per Cu atom, and they reported that the CO_2 molecule preferentially interacts with the coordinately unsaturated Cu site with a binding energy of −6.9 kcal mol^{-1}.[26,27] Recently, Kanoo et al.[28] investigated the absorption of CO_2 into the fluoro-functionalized PCP $\{[Zn(SiF_6)(Pz)_2]_2MeOH\}_n$ using the DFT-D method and reported that the CO_2 molecule occupies a central position of the unit cell in such a way that the C atom of CO_2 is surrounded by F atoms of four SiF_6 molecules. The calculated absorption enthalpy was quite large (−11.5 kcal mol^{-1}), which was attributed to the electrostatic interaction between the SiF_6 and CO_2 moieties. As shown by these works, the use of models consisting of both a metal and an organic linker is indispensible for the correct understanding of gas absorption into PCPs. Also, the factors determining the gas absorption site in PCPs have not been discussed at all to date, although knowledge of such factors is important for further development of this area.

Scheme 2. Realistic Model (RM) of the PCP with Adsorbed CS$_2$ (Fe, Green; Pt, Pink; N, Blue; C, Gray; S, Yellow)
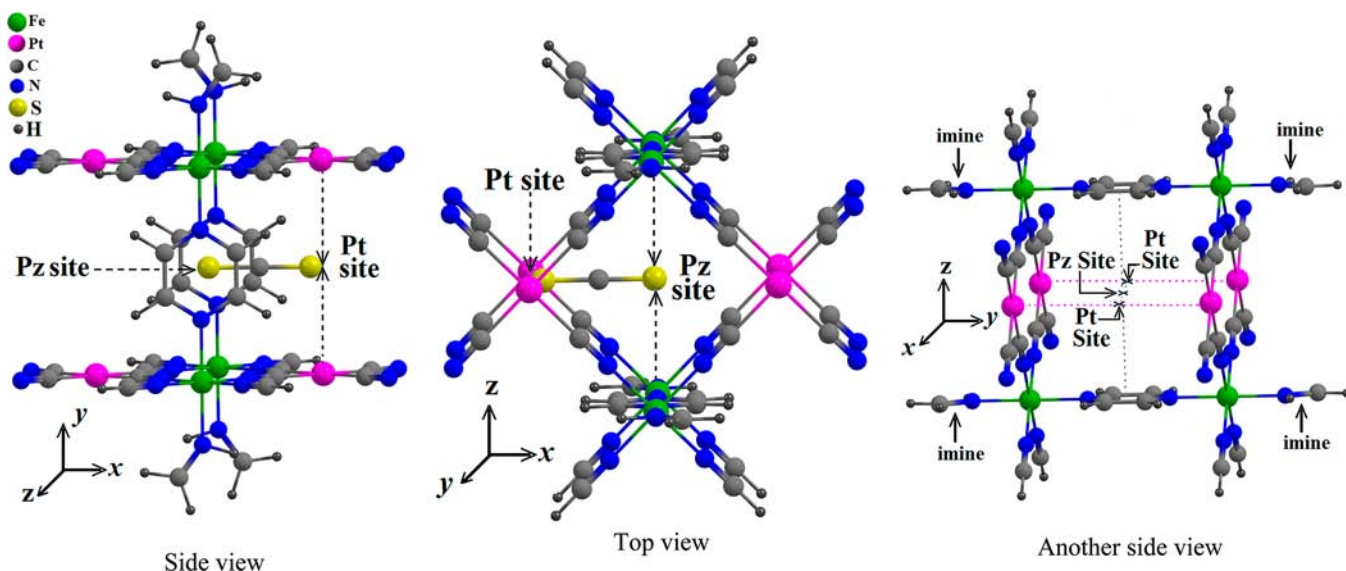
Scheme 3. Small Models (a) SM1 and (b) SM2 Used in the ONIOM Calculations, Representing the Pz and Pt Interaction Sites, Respectively

(a) Small model 1 (**SM1**) (b) Small model 2 (**SM2**)
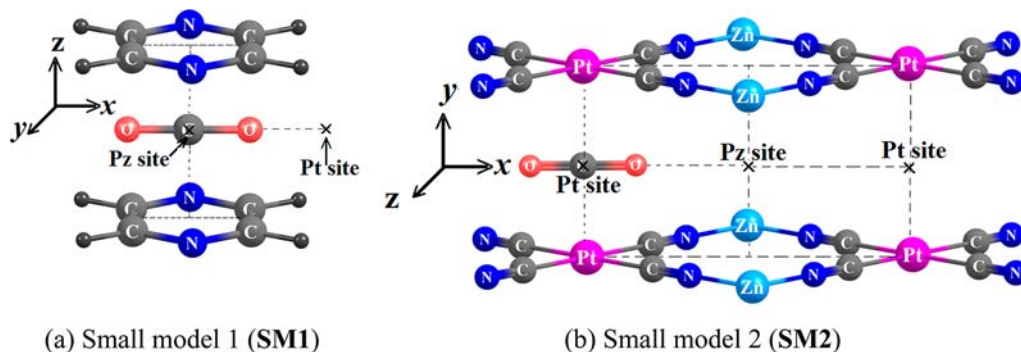
In this work, we theoretically investigated the interactions of CS$_2$ and CO$_2$ molecules using a realistic model consisting of a unit cell of $\{Fe^{II}(Pz)[Pt^{II}(CN)_4]\}_n$ in which both the metal and the organic linker were considered in the calculation. The purposes of the present work are to find the binding sites of these gas molecules in the Hofmann-type PCP, evaluate their binding energies, and clarify the factors determining the absorption sites and absorption energies of these molecules. We believe that such knowledge of determining factors is indispensible in understanding gas absorption into PCPs.

COMPUTATIONAL DETAILS AND MODELS

ONIOM Calculations and Models. The ONIOM method was employed in evaluating the absorption energies and absorption positions of CS$_2$ and CO$_2$ in the PCP. DFT was used for the low-level region, and the scaled MP2 methods SCS-MP2[29] and MP2.5 (the arithmetic mean of MP2 and MP3)[30] were used for the high-level regions. The ONIOM(MP2.5:DFT)-calculated binding energy was mainly used for the discussion because the MP2.5 method presents binding energies similar to those obtained using CCSD(T),[31] whereas the binding energy is overestimated in general by the MP2 method.[31] In the DFT calculations, the M06-2X functional was employed because this functional was suggested to evaluate the noncovalent interaction well.[32] The cc-pVTZ and aug-cc-pVTZ basis sets[33] were employed for C, N, O, S, and H in the low- and high-level regions of the ONIOM calculations, respectively. For Pt and Fe, the valence electrons were represented with (311111/22111/411) basis sets and

the core electrons were replaced by Stuttgart−Dresden−Born (SDB) effective core potentials (ECPs).[34] The LANL2DZ basis set was employed for the valence electrons of Zn, and its core electrons were replaced by the LANL2DZ ECP.[35] The counterpoise correction (CPC)[36] was made to account for basis-set superposition error (BSSE). The Gaussian 09 program package[37] was used in these calculations. Localized molecular orbital energy decomposition analysis (LMOEDA)[38] was performed using the GAMESS package.[39]

As shown in the X-ray structure of the PCP with absorbed CS$_2$ (Scheme 1), one of the two S atoms of CS$_2$ is found at a position intermediate between the centers of two Pz ligands and the other is intermediate between two Pt atoms. Considering the experimental structure of the PCP with absorbed CS$_2$, we employed the realistic model (**RM**) shown in Scheme 2. In this model, the CS$_2$ molecule is surrounded by two Pz ligands, 24 CN groups, four Fe atoms, and four Pt atoms and the terminal Pz ligands (which do not directly interact with the CS$_2$ molecule) are replaced with simple imine (Im) groups (H$_2$C=NH) to save computational cost. We ascertained that this substitution of Pz for the simple imine has very little influence on the binding energy, as discussed below. The geometrical parameters of **RM** were taken from the experimental structure in the low-spin state.[9a] As shown in Scheme 2, the interaction site between two Pz moieties is called a Pz site and that between two Pt atoms is called a Pt site. We also used the small models **SM1** and **SM2** for the ONIOM calculations. As shown in Scheme 3, **SM1** consists of two Pz molecules and **SM2** consists of four Pt(CN)$_4$ groups that are connected to four Zn atoms. In **SM2**, four Fe atoms were replaced with four Zn atoms to avoid a problem with 3d transition-metal

Scheme 4. Large Realistic Model (LRM) of the Hofmann-Type PCP (Fe, Green; Pt, Pink; N, Blue; C, Gray)

(A) Side View

(B) Top view
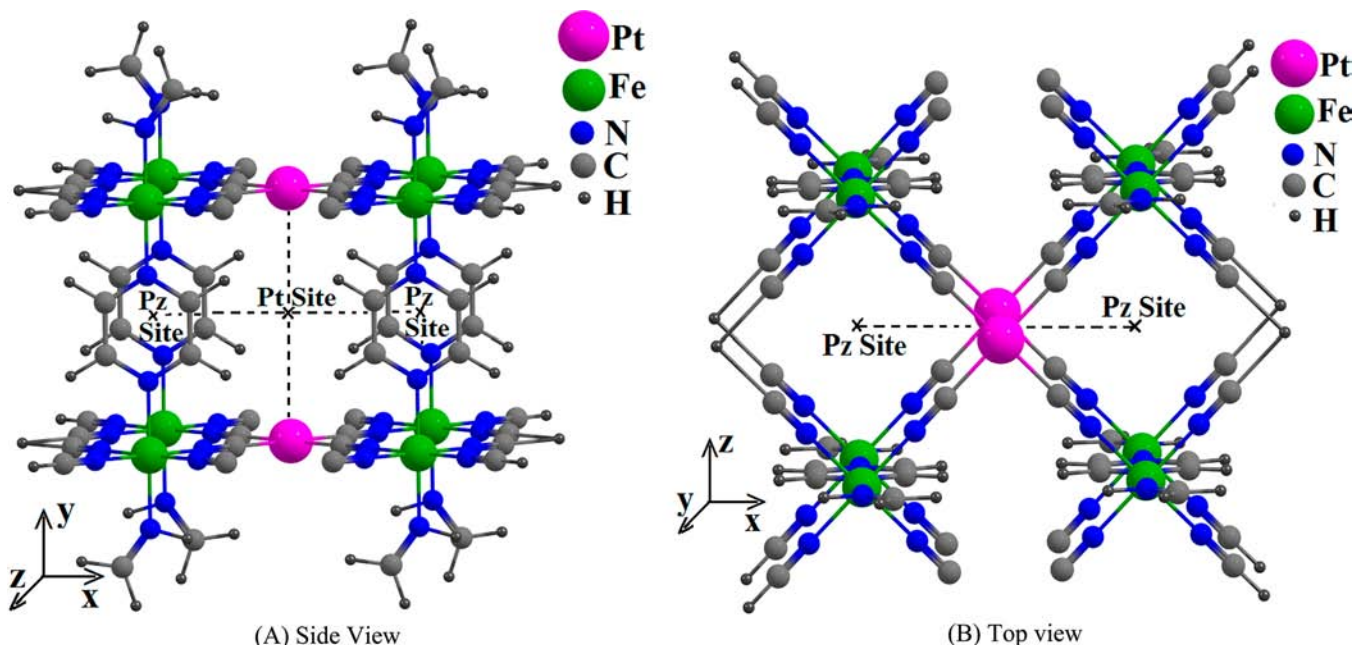
complexes in the MP2 calculation.[40] This substitution had little influence on the binding energy, as discussed below. In the case of the CO_2 absorption, we also used a large realistic model (**LRM**) (Scheme 4) because CO_2 takes a position at the edge of **RM**, as discussed below. **LRM** consists of eight Fe atoms, four Pz moieties, two Pt atoms, and 32 CN groups; the right- and left-hand sides of the Pt site are equivalent, as in the real structure (Scheme 1).

The binding energy (BE) of a gas molecule with **RM** (or **LRM**) was evaluated by the ONIOM scheme, as shown in eq 1:

$$\mathrm{BE}_{\mathbf{RM}}^{\mathrm{ONIOM}} = \mathrm{BE}_{\mathbf{RM}}^{\mathrm{low}} + \{\mathrm{BE}_{\mathbf{SM1}}^{\mathrm{high}} - \mathrm{BE}_{\mathbf{SM1}}^{\mathrm{low}}\} + \{\mathrm{BE}_{\mathbf{SM2}}^{\mathrm{high}} - \mathrm{BE}_{\mathbf{SM2}}^{\mathrm{low}}\}$$

(1)

where the superscripts "high" and "low" represent the high- and low-level calculations, respectively. The first term on the right-hand side of eq 1 is the binding energy of the gas molecule with **RM** (or **LRM**) calculated using the low-level computational method. This is a "real-low" component of the ONIOM scheme. The second and third terms (in braces) include the binding energies of the gas molecule with **SM1** and **SM2**, respectively, calculated using the high- and the low-level computational methods. After careful examinations, we selected the M06-2X functional with the cc-pVTZ basis set for the low-level calculations (see p S2 and Table S1 in the Supporting Information). For the high-level calculations, we mainly employed the MP2.5 method with aug-cc-pVTZ basis set (see p S2 in the Supporting Information). In the next section, we will also mention other ONIOM computational results such as ONIOM(SCS-MP2:M06-2X), ONIOM-(MP2:M06-2X), and ONIOM(MP2.5:Hartree−Fock) in discussing the reliability of the ONIOM scheme.

Tests of the Model Systems. First, we wish to discuss briefly the reliability of the model systems. One important modification was the substitution of terminal Pz with Im in **RM** and **LRM**. To check the influence of this substitution, the two model systems $[(\mathrm{Pz})\mathrm{Fe}(\mathrm{CNH})_4-\mathrm{Pz}-\mathrm{Fe}(\mathrm{CNH})_4(\mathrm{Pz})]$ and $[(\mathrm{Im})\mathrm{Fe}(\mathrm{CNH})_4-\mathrm{Pz}-\mathrm{Fe}-(\mathrm{CNH})_4(\mathrm{Im})]$ (Supporting Information Figure S1) were examined by the DFT method with the M06-2X functional, and little differences between their CO_2 binding energies and d-orbital populations were found (Supporting Information Table S2). Another modification was the substitution of Fe with Zn in **SM2** (see Scheme 3). We calculated the binding energies of CO_2 with $[(\mathrm{Im})\mathrm{Fe}(\mathrm{CNH})_4(\mathrm{Pz})]$ and its Zn analogue using DFT(M06-2X) and found little difference between them (Supporting Information Figure S2). These results suggest that the substitutions of terminal Pz and Fe with Im and Zn, respectively,

have little influence on the binding energies of the gas molecules with this PCP.

RESULTS AND DISCUSSION

Absorption Positions of CO_2 and CS_2 in the PCP and Their Absorption Energies. To find the absorption position of CS_2 molecule in the PCP, a potential energy surface (PES) was scanned by moving the CS_2 molecule along the line connecting the Pz and Pt sites (Figure 1). The coordinate R_1 in
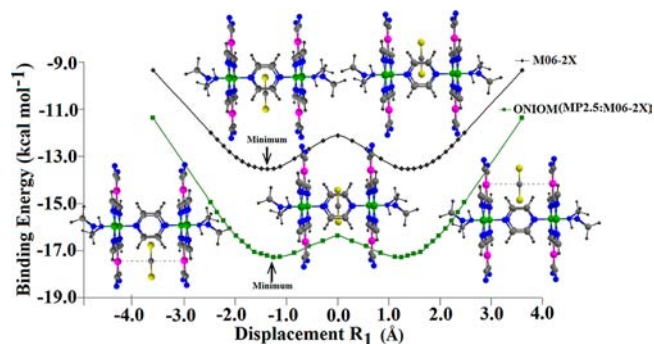

Figure 1. DFT(M06-2X)- and ONIOM(MP2.5:M06-2X)-calculated potential energy surfaces for CS_2 absorption in the PCP. Displacement R_1 is along the x axis (see Scheme 2).

Figure 1 represents the position of C of CS_2, with the Pz site defined as the origin ($R_1 = 0.0$ Å). The Pt site corresponds to the position $R_1 = 3.6$ Å. The ONIOM(MP2.5:M06-2X) method provided a minimum at $R_1 = 1.37$ Å. At this minimum position, one of the two S atoms of CS_2 is found at the Pz site and the other is at the Pt site. This optimized position agrees with the experimental geometry.[9a] Hereafter, this position ($R_1 = 1.37$ Å) is called the CS_2 minimum position or simply the CS_2 position. We also investigated the minimum with other computational methods in the ONIOM calculation, and all of them provided almost the same minimum position (see pp S5 and S6 and Figure S3 in the Supporting Information). The

binding energy of CS_2 at this minimum position was calculated to be -17.3 kcal mol^{-1} using ONIOM(MP2.5:M06-2X), as shown in Table 1; for a discussion of the binding energies

Table 1. ONIOM(MP2.5:M06-2X)-Calculated Binding Energies (in kcal mol^{-1}) of Gas Molecules at the CO_2 and CS_2 Positions

real	SM1		SM2		
low[a,b]	low[a,b]	high[a,c]	low[a,b,d]	high[a,c,d]	ONIOM
M06-2X	M06-2X	MP2.5	M06-2X	MP2.5	(M06-2X:MP2.5)
		CS_2 Absorption at the CO_2 Position			
-9.33	-1.42	-2.85	-8.94	-9.55	-11.37
		CS_2 Absorption at the CS_2 Position			
-13.52	-4.02	-5.47	-9.07	-11.39	-17.29
		CO_2 Absorption at the CO_2 Position			
-4.67	-0.04	-0.68	-4.52	-4.38	-5.17
		CO_2 Absorption at the CS_2 Position			
-3.11	-2.58	-3.35	-0.05	-0.92	-4.75

[a]The (311111/22111/411) basis set was employed for the Pt and Fe valence electrons, and their core electrons were replaced by SDB ECPs. [b]The cc-pVTZ basis set was used for H, C, N, O, and S. [c]The aug-cc-pVTZ basis set was used for H, C, N, O, and S. [d]The LANL2DZ basis set was employed for the Zn valence electrons, and the core electrons were replaced by the LANL2DZ ECP.

obtained from the other ONIOM calculations (see p S9 and Tables S3 and S4 in the Supporting Information). We also examined the movements along the y and z axes but found the minimum at $R_y = 0.0$ and $R_z = 0.0$ (see Supporting Information Figures S6 and S7, respectively).

Interestingly, the PES of the CO_2 absorption (Figure 2) is completely different from that of the CS_2 absorption (Figure 1)
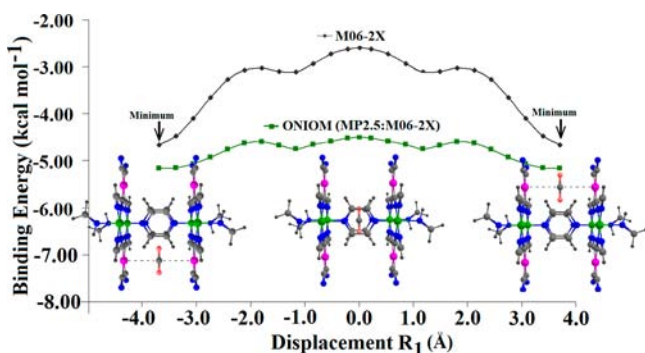

Figure 2. DFT(M06-2X)- and ONIOM(MP2.5:M06-2X)-calculated potential energy surfaces for CO_2 absorption in the PCP. Displacement R_1 is along the x axis (see Scheme 2).

in the following ways: (i) the minimum was found at $R_1 = 3.6$ Å, where the C atom of CO_2 is located at the Pt site; (ii) the Pz site (near $R_1 = 0.0$ Å) is less favorable; (iii) the binding energy of CO_2 is considerably smaller than that of CS_2, and the PES is very shallow.[41] It should be noted in Figure 2 that this minimum was found at the edge of **RM** ($R_1 = 3.6$ Å). At this position, the interaction of CO_2 with the Pt site is not considered very well; in one direction with $R_1 < 3.6$ Å, there are two Pz molecules, but in the other direction with $R_1 > 3.6$ Å, there is no Pz molecule. In other words, for **RM** the situation is different on either side of $R_1 = 3.6$ Å. In this regard, **RM** is not a good model of the real PCP (Scheme 1) in the case of CO_2

absorption. To avoid this problem, we employed the larger realistic model **LRM** (Scheme 4). As shown in Figure 3, the
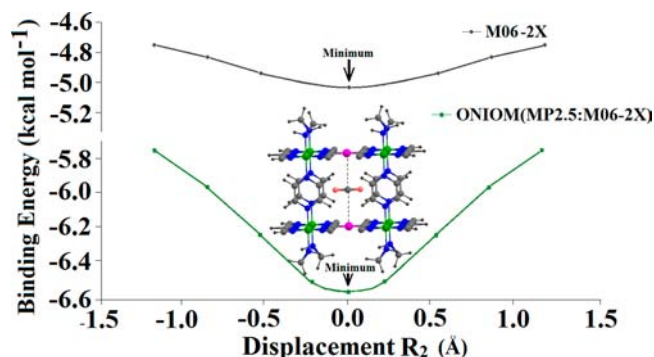

Figure 3. DFT(M06-2X)- and ONIOM(MP2.5:M06-2X)-calculated potential energy surfaces for CO_2 absorption in the PCP. The large realistic model (**LRM**) was employed. Displacement R_2 is along the x axis (see Scheme 4); the origin $R_2 = 0.0$ Å corresponds to the Pt site.

origin $R_2 = 0.0$ Å corresponds to the structure in which the C atom of CO_2 is at the Pt site. Apparently, the ONIOM-(MP2.5:M06-2X) method provides a minimum at $R_2 = 0.0$ Å, which corresponds to the position $R_1 = 3.6$ Å in Figure 2. On the basis of these results, it is concluded that CO_2 absorption occurs at the Pt site in this PCP. Hereafter, this position ($R_1 = 3.6$ Å in Figure 2) is called the CO_2 minimum position or simply the CO_2 position.

The binding energy of CO_2 at the CO_2 position was calculated to be -5.2 kcal mol^{-1} by the ONIOM(MP2.5:M06-2X) method. This binding energy is much smaller than that of CS_2. The larger binding energy and deeper PES of CS_2 in comparison with CO_2[41] are consistent with the facts that CS_2 was observed in the PCP by X-ray crystallography but CO_2 was not.[9a] These results suggest that the CS_2 molecule does not move easily but the CO_2 does move easily in the PCP. The ONIOM calculations with other computational methods also provided a similar minimum position (see pp S13−S18 and Tables S4 and S5 in the Supporting Information). Another important result here is that the binding energy of CS_2 is much larger than the rotational barrier of the Pz ring ($\sim$6 kcal mol^{-1}),[9b] which is enough to suppress the rotational movement of the Pz ligand. However, the binding energy of CO_2 is smaller than the rotational barrier, indicating that the CO_2 absorption cannot suppress the rotation of the Pz ligand. Also, it is distant from the Pz ligand, which is not favorable for suppressing the Pz rotation.

Contributions of the Pz and Pt Moieties to the Binding Energy. It is of considerable interest to elucidate the factors determining the absorption position of gas molecule. We recently reported that the dispersion interaction is important in the binding energy of a gas molecule with two Pz molecules.[31] Considering the importance of the dispersion interaction (E_{DIS}), it is reasonable to discuss separately the contributions of E_{DIS} and other interactions to the binding energy. Thus, we investigated the binding energy at the Hartree−Fock level (BE$_{HF}$) and the contribution of electron correlation to the binding energy using the small models **SM1** and **SM2**. It is noted that the sum of the MP2.5-calculated binding energies for **SM1** and **SM2** presents a minimum at $R_1 = 1.49$ Å in the CS_2 absorption, which is close to the ONIOM(MP2.5:M06-2X)-calculated minimum position for

RM ($R_1 = 1.37$ Å) (Figure 4C). This result indicates that the analysis of the PES can be successfully made with **SM1** and **SM2**.
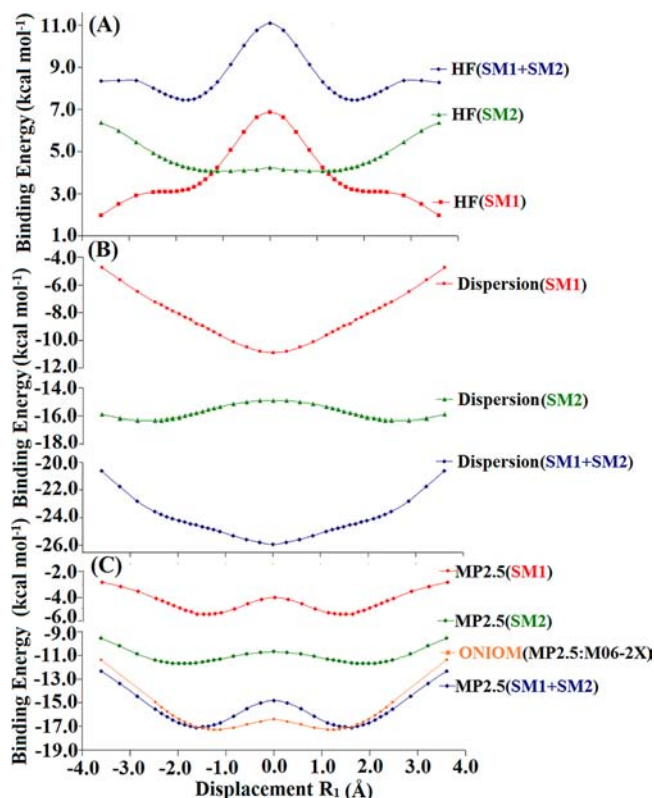

Figure 4. Hartree−Fock (HF)- and MP2.5-calculated potential energy surfaces for CS_2 absorption with **SM1** and **SM2**. Displacement R_1 is along the x axis (see Scheme 3).

As shown in Figure 4A, the BE_{HF} for CS_2 with **SM1** is very repulsive at $R_1 = 0.0$ Å but less repulsive at $R_1 = 3.6$ Å, while the BE_{HF} with **SM2** is less repulsive at $R_1 = 0.0$ Å and more repulsive at $R_1 = 3.6$ Å. Their sum is repulsive at $R_1 = 0.0$ Å and presents a minimum around $R_1 = 1.74$ Å. E_{DIS} for **SM1** presents a minimum at $R_1 = 0.0$ Å but considerably increases with increasing R_1 (Figure 4B). On the other hand, E_{DIS} for **SM2** exhibits a moderate dependence on R_1. Though the E_{DIS} largely contributes to the binding energy at $R_1 = 0.0$ Å, its stabilization is almost overcome by the large destabilization by the BE_{HF} term at this position. Around $R_1 = 1.49$ Å, the sum of the BE_{HF} values with **SM1** and **SM2** is moderately repulsive, but E_{DIS} for **SM1** is considerably attractive. Hence, $R_1 = 1.49$ Å rather than $R_1 = 0.0$ Å becomes a minimum because of the balance between BE_{HF} and E_{DIS}. In other words, the Pz site (near $R_1 = 0.0$ Å) is unfavorable because of the large destabilization energy with **SM1** at the HF level, but the Pt site (near $R_1 = 3.6$ Å) is also unfavorable because of the very small contribution of the dispersion interaction of **SM1**. As a result, the position around $R_1 = 1.49$ Å becomes the minimum.

For CO_2 absorption, the sum of the BEs with **SM1** and **SM2** exhibits a PES similar to the ONIOM(MP2.5:M06-2X)-calculated one (Figure 5C). It is noted that the PESs with **SM1** and **SM2** for CO_2 absorption are much different from those for CS_2 absorption, like that of the ONIOM-calculated PES. The BE_{HF} of **SM1** does not show considerably large destabilization at $R_1 = 0.0$ Å, and it depends much less on R_1
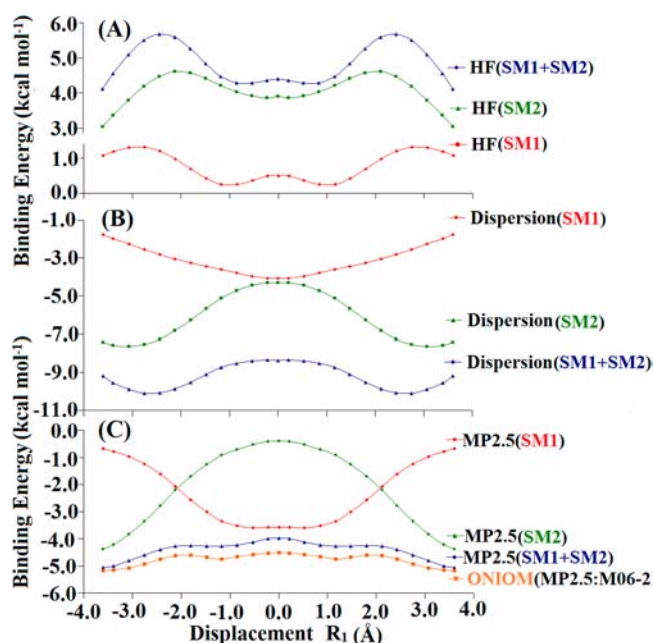

Figure 5. Hartree−Fock (HF) and MP2.5-calculated potential energy surfaces for CO_2 absorption with **SM1** and **SM2**. Displacement R_1 is along the x axis (see Scheme 3).

than in the CS_2 case (Figure 5A). The BE_{HF} of **SM2** shows a minimum around $R_1 = 3.6$ Å, unlike the CS_2 case. Their sum is as stable at $R_1 = 0.0$ Å as at $R_1 = 3.6$ Å but exhibits somewhat large destabilization at $R_1 = 2.4−2.8$ Å (Figure 5A). The E_{DIS} stabilization for **SM2** is much larger at $R_1 = 2.75$ Å than at $R_1 = 0.0$ Å, while that for **SM1** is moderately larger at $R_1 = 0.0$ Å than at $R_1 = 2.75$ Å (Figure 5B). As a result, for E_{DIS}, the Pz site ($R_1 = 0.0$ Å) is unfavorable but the position around $R_1 = 2.75$ Å becomes favorable. However, the destabilization at the HF level is quite large around $R_1 = 2.75$ Å, which cancels out the stabilization by E_{DIS}. Hence, this position ($R_1 = 2.75$ Å) does not become a minimum. On the other hand, the BE_{HF} values are similar at $R_1 = 3.6$ Å and 0.0 Å and the sum of the E_{DIS} values for **SM1** and **SM2** is more negative at $R_1 = 3.6$ Å than at $R_1 = 0.0$ Å. As a result, the position $R_1 = 3.6$ Å becomes the minimum.

In conclusion, the balance between the stabilizing E_{DIS} term and the destabilizing BE_{HF} determines the absorption position of CS_2 at $R_1 = 1.49$ Å and that of CO_2 at $R_1 = 3.60$ Å. We wish to further explore these results by performing an energy decomposition analysis of BE_{HF}.

The Reason Why CS_2 Takes an Intermediate Position between the Pz and Pt Sites but CO_2 Takes a Position at the Pt Site. It is of considerable interest to elucidate the reasons why the C atom of CS_2 takes an intermediate position between the Pz and Pt sites ($R_1 = 1.37$ Å) but that of CO_2 takes a position at the Pt site ($R_1 = 3.6$ Å). For this purpose, the binding energies of the gas molecules with **SM1** and **SM2** were analyzed at the CS_2 position ($R_1 = 1.37$ Å) and the CO_2 position ($R_1 = 3.6$ Å). The localized molecular orbital energy decomposition analysis was carried at the HF level.[38] As shown in Table 2, the electrostatic (ES), exchange repulsion (EXR), and dispersion (DIS) interactions mainly contribute to the total binding energy, but the charge transfer (CT) + polarization (POL) + coupling (MIX) term contributes moderately. These results are consistent with our expectation that a noncovalent

Table 2. Contributions of Various Interaction Terms to the Absorption Energies (in kcal mol⁻¹) of CO_2 and CS_2 Molecules with the PCP

gas position	SM1					SM2				
	ES	EXR	CT+POL+MIX	HF	DIS	ES	EXR	CT+POL+MIX	HF	DIS
CO_2 Absorption										
CS_2 position (R_1 = 1.37 Å)	−1.33	1.85	−0.18	0.34	−3.64	1.98	2.79	−0.55	4.21	−5.13
CO_2 position (R_1 = 3.60 Å)	0.54	0.60	−0.076	1.08	−1.76	−2.08	6.59	−1.47	3.04	−7.59
CS_2 Absorption										
CS_2 position (R_1 = 1.37 Å)	−3.08	7.62	−0.61	3.93	−9.40	−8.56	15.91	−3.29	4.07	−15.47
CO_2 position (R_1 = 3.60 Å)	−1.63	4.05	−0.51	1.91	−4.70	−7.05	17.48	−4.08	6.37	−15.92

interaction is mainly formed between the gas molecule and the PCP.

For CO_2 absorption, the sum of the DIS interactions for **SM1** and **SM2** is moderately larger and that of the ES terms for **SM1** and **SM2** is considerably larger at the CO_2 position than at the CS_2 position (Table 2). On moving from the CS_2 position to the CO_2 position, the EXR destabilization somewhat increases. However, the ES contribution increases more than the EXR destabilization, and the CT+POL+MIX and DIS terms also moderately increase on moving from the CS_2 position to the CO_2 position. As a result, CO_2 takes the position at the Pt site (R_1 = 3.6 Å). It should be noted that the ES stabilization increases much more than the DIS and CT +POL+MIX terms when going from the CS_2 position to the CO_2 position and that **SM2** rather than **SM1** mainly contributes to the ES stabilization of the CO_2 position (Table 2). On the basis of these results, it is concluded that the ES interaction plays an important role in determining the absorption position of CO_2; in particular, the Pt moiety (**SM2**) mainly contributes to the ES stabilization.

For CS_2 absorption, the sum of the ES stabilizations for **SM1** and **SM2** is moderately larger at the CS_2 position than at the CO_2 position by 3 kcal mol⁻¹. The sum of the EXR destabilizations for **SM1** and **SM2** is slightly larger at the CS_2 position than at the CO_2 position by ~1.5 kcal mol⁻¹. Though E_{DIS} for **SM2** is similar for the CS_2 and the CO_2 positions, E_{DIS} for **SM1** is much larger at the CS_2 position than at the CO_2 position by 5.0 kcal mol⁻¹. As a result, CS_2 takes the position R_1 = 1.37 Å. At this position, the DIS term considerably contributes and the ES term moderately contributes to the overall stabilization. It should be noted that the DIS stabilization of **SM1** increases much more than other terms in going from the CO_2 position to the CS_2 position. This leads to the conclusion that the DIS term of **SM1** plays an important role in determining the position of the CS_2 absorption.

Reasons Why the Electrostatic Interaction Is Important for CO_2 Absorption and the Dispersion Interaction Is Important for CS_2 Absorption. To understand the electrostatic interactions at the CO_2 and CS_2 positions, the electrostatic potential was calculated with **LRM**. In Figure 6a,b, the electrostatic potential is mapped on two different planes, the plane parallel to two Pz rings and passing through two Pt centers (Figure 6a) and that parallel to two Pt(CN)₄ planes and passing through the centers of two Pz rings (Figure 6b). In these maps, the blue and red colors correspond to electronegative and electropositive regions, respectively. As can be seen in Figure 6, the electronegative regions appear around the Pt site; it should be remembered that the Pt site is not the Pt atom itself but the position between two Pt atoms. Thus, the electrostatic stabilization is large when a positively charged species takes the position near the Pt site. We also calculated
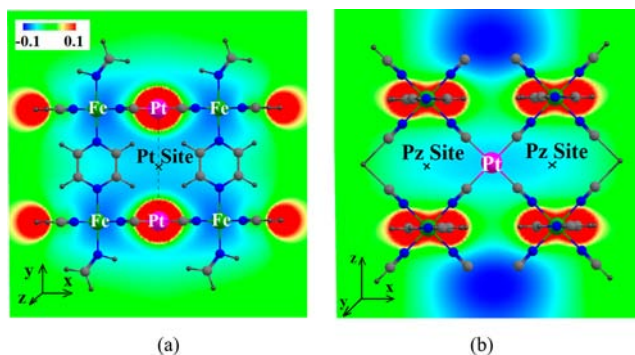

Figure 6. Electrostatic potential of the **LRM** framework in (a) the plane parallel to two Pz rings and passing through two Pt centers and (b) the plane parallel to two Pt centers and passing through Pz rings (see Scheme 4). The M06-2X level of theory was employed. In (a), there are two Pt atoms in the plane, two Pz rings above the plane, and two Pz rings below the plane. In (b), one Pt atom is above the plane and the other Pt atom is below the plane. Also see Scheme 4.

the electrostatic potential along the x axis between R_1 = 0.0 Å and R_1 = 3.6 Å (see Scheme 2 for the x axis). In Figure 7a, R_1 =
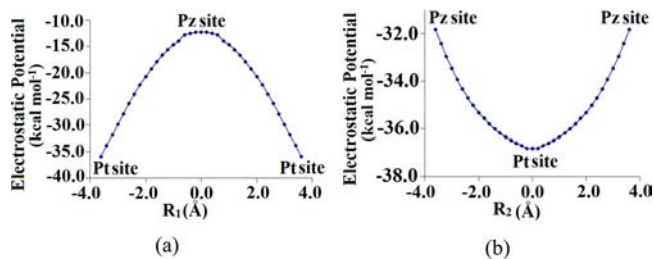

Figure 7. Electrostatic potential along the x axis (see Schemes 2 and 4 for details of the x, y, and z coordinates) using (a) **RM** (R_1 = 0.00 and 3.60 Å represent the Pz and Pt sites, respectively; see Scheme 2) and (b) **LRM** (R_2 = 0.00 and 3.60 Å represent the Pt and Pz sites, respectively; see Scheme 4). The M06-2X functional was employed.

0.0 Å corresponds to the Pz site and R_1 = 3.6 Å corresponds to the Pt site, where **RM** was employed. For a better representation of the electrostatic potential at R_1 = ±3.6 Å, we also calculated the electrostatic potential with **LRM** (Figure 7b). This is because the electrostatic potential around the Pz site is correctly represented with **RM** and that around the Pt site is correctly represented with **LRM**, as discussed above (see Schemes 2 and 3 for **RM** and **LRM**, respectively). On the basis of Figure 7, it is concluded that the electrostatic potential is the most negative at the Pt site and becomes less negative in going from the Pt site to the Pz site. Scheme 5 shows the quadrupole moments and natural bond orbital (NBO) atomic charges of CO_2 and CS_2 molecules. Some important findings are

Scheme 5. Schematic Representation of the Electric Quadrupole Moments (Q) and NBO Atomic Charges of CO_2 and CS_2 Molecules
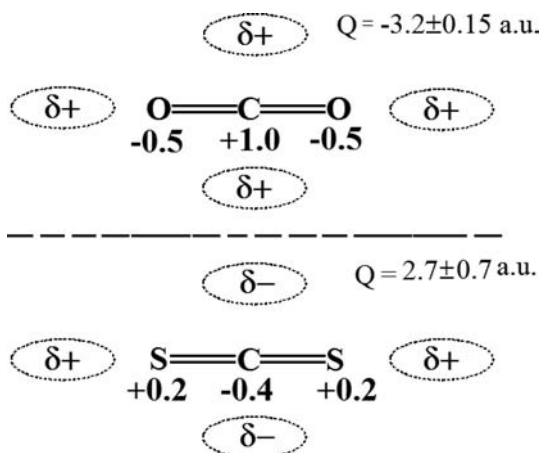
summarized as follows: (1) the C atom is much more positively charged in CO_2 than in CS_2; (2) the O atom in CO_2 is more negatively charged than the S in CS_2; and (3) the quadrupole moment of CO_2 is somewhat larger than that of CS_2, and its sign is opposite to that of CS_2. From the quadrupole moments and atomic charges of the gas molecules and the electrostatic potential of the framework (Figures 6 and 7), it is concluded that in CO_2 absorption, the electrostatic stabilization is the largest when the C atom of CO_2 takes the position at the Pt site but becomes smaller as it moves toward the Pz site. The electrostatic interaction of CS_2 with the PCP follows the opposite trend and changes much less than in the case of CO_2 when going from the CO_2 position to the CS_2 position. This occurs because the quadrupole moment and the positive charge of the C atom are smaller in CS_2 than in CO_2.

The dispersion interaction is correlated to the z component of the polarizability of the gas molecule[31] (see Scheme 2 for the z axis). The z component of the polarizability of CS_2 (8.74 Å^3) is much larger than that of CO_2 (2.65 Å^3). Because of this large polarizability, the dispersion interaction of CS_2 with the PCP is much larger than that of CO_2. In going from the CS_2 position to the CO_2 position, CS_2 completely leaves the region between two Pz molecules of **SM1** (see Scheme 2). This movement induces a significantly large decrease in the dispersion interaction with **SM1**, as clearly displayed in Table 2. However, CS_2 does not completely leave the region between two $Pt(CN)_4$ moieties in **SM2** when moving from the Pz site to the Pt site (see Scheme 2). Thus, the dispersion interaction of CS_2 is much more sensitive to **SM1** than to **SM2**. It is concluded that the dispersion interaction with **SM1** is an important factor in determining the CS_2 absorption position.

In conclusion, the dispersion interaction between CS_2 and two Pz molecules plays an important role in determining the CS_2 absorption position. For CO_2 absorption, on the other hand, the dispersion interaction is intrinsically small and hence changes much less than that of CS_2 as CO_2 moves from the CS_2 position to the CO_2 position. In other words, the dispersion interaction is not a determining factor for the CO_2 position.

CONCLUDING REMARKS

The absorption of CO_2 and CS_2 molecules into the Hofmann-type three-dimensional PCP $\{Fe(Pz)[Pt(CN)_4]\}_n$ (Pz = pyrazine) was studied theoretically in the present work, mainly

using the ONIOM(MP2.5:M06-2X) method. The binding energies and potential energy surfaces were scanned by displacing the gas molecule along the x axis connecting the Pz and the Pt sites. The PES for CO_2 absorption is shallow but that for CS_2 is deep, suggesting that CO_2 moves easily in the PCP but CS_2 does not. The ONIOM calculations clearly show that CO_2 is weakly absorbed at the Pt site but that CS_2 is strongly absorbed between the Pz and Pt sites. The calculated absorption position of CS_2 agrees with the X-ray structure of the PCP containing absorbed CS_2.[9a] To determine the reasons why the absorption positions and stabilization energies of CO_2 and CS_2 are different, an energy decomposition analysis was carried out at the HF level. It is concluded that the CO_2 absorption is considerably stabilized by the electrostatic interaction with the $Pt(CN)_4$ moiety and the CS_2 absorption is considerably stabilized by the dispersion interaction with two Pz molecules. Analyzing differences in the quadrupole moments, atomic charges, and polarizabilities of CO_2 and CS_2, we found that in the CO_2 absorption, the electrostatic stabilization is large when the C atom of CO_2 is located at the Pt site. The dispersion interaction of CS_2 is considerably larger than that of CO_2 because the polarizability of CS_2 is much larger than that of CO_2. In particular, the dispersion interaction with two Pz molecules is important in determining the CS_2 position, because two Pz molecules induce a considerably large dispersion interaction when the gas molecule exists between them but not when the gas molecule leaves the region between them.

These successful explanations are meaningful not only for CO_2 and CS_2 absorption into the Hofmann-type PCP but also for the absorption of other gas molecules. For instance, in the case of gas molecules having a quadrupole moment and charge distribution similar to those of CO_2, the absorption should occur at the Pt site. On the other hand, for gas molecules having a large polarizability and a quadrupole moment similar to those of CS_2, the CS_2 position would be favorable for the absorption. Such gas molecules should induce the spin transition from the high-spin to the low-spin state. Also, the present analysis with the important fragments such as **SM1** and **SM2** provides clear insights into the absorption of gas molecules into the PCP. We wish to emphasize that this type of analysis is useful for gas absorption in various PCPs.

ASSOCIATED CONTENT

Ⓢ Supporting Information

Geometries of the model systems (Figures S1 and S2); PESs of CS_2 with **RM** (Figures S3, S6, and S7), **SM1** (Figure S4), and **SM2** (Figure S5); PESs of CO_2 with **RM** (Figure S8), **LRM** (Figure S11), **SM1** (Figure S9), and **SM2** (Figure S10); binding energies of various gas molecules with two Pz molecules (Table S1); binding energies of CO_2 with the model systems (Table S2); and binding energies of CS_2 and CO_2 at different positions on the DFT(M062X) and ONIOM PESs (Tables S3−S5). This material is available free of charge via the Internet at http://pubs.acs.org.

AUTHOR INFORMATION

Corresponding Author

sakaki.shigeyoshi.47e@st.kyoto-u.ac.jp

Notes

The authors declare no competing financial interest.

REFERENCES

(1) (a) Sumida, K.; Rogow, D. L.; Mason, J. A.; McDonald, T. M.; Bloch, E. D.; Herm, Z. R.; Bae, T. H.; Long, J. R. *Chem. Rev.* **2012**, *112*, 724. (b) Suh, M. P.; Park, H. J.; Prasad, T. K.; Lim, D. W. *Chem. Rev.* **2012**, *112*, 782. (c) Murray, L. J.; Dincă, M.; Long, J. R. *Chem. Soc. Rev.* **2009**, *38*, 1294. (d) Morris, R. E.; Wheatley, P. S. *Angew. Chem., Int. Ed.* **2008**, *47*, 4966.

(2) For work on both gas storage and separation, see: (a) Kim, K.; Banerjee, M.; Yoon, M.; Das, S. *Top. Curr. Chem.* **2010**, *293*, 115. (b) Czaja, A. U.; Trukhan, N.; Muller, U. *Chem. Soc. Rev.* **2009**, *38*, 1284. (c) Kitagawa, S.; Matsuda, R. *Coord. Chem. Rev.* **2007**, *251*, 2490. (d) James, S. L. *Chem. Soc. Rev.* **2003**, *32*, 276.

(3) (a) Gong, Q.; Olson, D. H.; Li, J. *Chem. Rev.* **2012**, *112*, 836. (b) Li, J. R.; Sculley, J.; Zhou, H.-C. *Chem. Rev.* **2012**, *112*, 869. (c) Li, J.-R; Kuppler, R. J.; Zhou, H.-C. *Chem. Soc. Rev.* **2009**, *38*, 1477. (d) Nanoporous and Nanostructured Materials for Catalysis Sensor and Gas Separation Applications. Materials Research Society 2005 Spring Meeting, San Francisco, CA, March 28−31, 2005; Symposium R.

(4) (a) Yoon, M.; Srirambalaji, R.; Kim, K. *Chem. Rev.* **2012**, *112*, 1196. (b) Corma, A.; García, H.; Llabrés i Xamena, F. X. *Chem. Rev.* **2010**, *110*, 4606. (c) Lee, J.; Farha, O. K.; Roberts, J.; Scheidt, K. A.; Nguyen, S. T.; Hupp, J. T. *Chem. Soc. Rev.* **2009**, *38*, 1450. (d) Ma, L. Q.; Abney, C.; Lin, W. B. *Chem. Soc. Rev.* **2009**, *38*, 1248. (e) Wang, Z.; Chen, G.; Ding, K. *Chem. Rev.* **2009**, *109*, 322. (f) Farrusseng, D.; Aguado, S.; Pinel, C. *Angew. Chem., Int. Ed.* **2009**, *48*, 7502.

(5) (a) Zhou, H.-C.; Long, J. R.; Yaghi, O. M. *Chem. Rev.* **2012**, *112*, 673. (b) O'Keefe, M.; Yaghi, O. M. *Chem. Rev.* **2012**, *112*, 675. (c) Sanchez, C.; Shea, K. J.; Kitagawa, S. *Chem. Soc. Rev.* **2011**, *40*, 471. (d) Seo, J.; Sakamoto, H.; Matsuda, R.; Kitagawa, S. *J. Nanosci. Nanotechnol.* **2010**, *10*, 3. (e) Perry, J. J., IV; Perman, J. A.; Zaworotko, M. J. *Chem. Soc. Rev.* **2009**, *38*, 1400. (f) Tranchemontagne, D. J.; Mendoza-Cortés, J. L.; O'Keeffe, M.; Yaghi, O. M. *Chem. Soc. Rev.* **2009**, *38*, 1257. (g) Suh, M. P.; Cheon, Y. E.; Lee, E. Y. *Coord. Chem. Rev.* **2008**, *252*, 1007.

(6) (a) Cheon, Y. E.; Suh, M. P. *Chem. Commun.* **2009**, 2296. (b) Britt, D.; Tranchemontagne, D.; Yaghi, O. M. *Proc. Natl. Acad. Sci. U.S.A.* **2008**, *105*, 11623. (c) Mulfort, K. L.; Hupp, J. T. *J. Am. Chem. Soc.* **2007**, *129*, 9604.

(7) (a) Zhang, W.; Xiong, R.-G. *Chem. Rev.* **2012**, *112*, 1163. (b) Weng, D. F.; Wang, Z. M.; Gao, S. *Chem. Soc. Rev.* **2011**, *40*, 3157. (c) Dechambenoit, P.; Long, J. R. *Chem. Soc. Rev.* **2011**, *40*, 3249. (d) Kurmoo, M. *Chem. Soc. Rev.* **2009**, *38*, 1353. (e) Tanaka, D.; Horike, S.; Kitagawa, S.; Ohba, M.; Hasegawa, M.; Ozawa, Y.; Toriumi, K. *Chem. Commun.* **2007**, 3142.

(8) (a) Cui, Y.; Yue, Y.; Qian, G.; Chen, B. *Chem. Rev.* **2012**, *112*, 1126. (b) Rocha, J.; Carlos, L. D.; Paz, F. A. A.; Ananias, D. *Chem. Soc. Rev.* **2011**, *40*, 926. (c) Allendorf, M. D.; Bauer, C. A.; Bhakta, R. K.; Houk, R. J. T. *Chem. Soc. Rev.* **2009**, *38*, 1330.

(9) (a) Ohba, M.; Yoneda, K.; Agustí, G.; Muñoz, M. C.; Gaspar, A. B.; Real, J. A.; Yamasaki, M.; Ando, H.; Nakao, Y.; Sakaki, S.; Kitagawa, S. *Angew. Chem., Int. Ed.* **2009**, *48*, 4767. (b) Ando, H.; Nakao, Y.; Sato, H.; Ohba, M.; Sakaki, S.; Kitagawa, S. *Chem. Phys. Lett.* **2011**, *511*, 399.

(10) Bao, X.; Shepherd, H. J.; Salmon, L.; Molnár, G.; Tong, M.-L.; Bousseksou, A. *Angew. Chem., Int. Ed.* **2013**, *52*, 1198.

(11) (a) Kreno, L. E.; Leong, K.; Farha, O. K.; Allendorf, M.; Van Duyne, R. P.; Hupp, J. T. *Chem. Rev.* **2012**, *112*, 1105. (b) Lefebvre, J.; Korčok, J. L.; Katz, M. J.; Leznoff, D. B. *Sensors* **2012**, *12*, 3669. (c) Ohmori, O.; Kawano, M.; Fujita, M. *Angew. Chem., Int. Ed.* **2005**, *44*, 1962. (d) Ruben, M.; Rojo, J.; Romero-Salguero, F. J.; Uppadine, L. H.; Lehn, J.-M. *Angew. Chem., Int. Ed.* **2004**, *43*, 3644. (e) Halder, G. J.; Kepert, C. J.; Moubaraki, B.; Murray, K. S.; Cashion, J. D. *Science* **2002**, *298*, 1762.

(12) (a) Zhang, J.-P.; Zhang, Y.-B.; Lin, J.-B. ; Chen, X.-M. *Chem. Rev.* **2012**, *112*, 1001. (b) Shongwe, M. S.; Al-Rahbi, S. H.; Al-Azani, M. A.; Al-Muharbi, A. A.; Al-Mjeni, F.; Matoga, D.; Gismelseed, A.; Al-Omari, I. A.; Adams, H.; Morris, M. J.; Mikuriya, M. *Dalton Trans.* **2012**, *41*, 2500. (c) Cingolani, A.; Galli, S.; Masciocchi, N.; Pandolfo, L.; Pettinari, C.; Sironi, A. *J. Am. Chem. Soc.* **2005**, *127*, 6144. (d) Dong, Y. B.; Zhao, X.; Tang, B.; Wang, H. Y.; Huang, R. Q.; Smith, M. D.; Loye, H. C. *Chem. Commun.* **2004**, 220.

(13) Hauser, A. *Top. Curr. Chem.* **2004**, *233*, 49.

(14) (a) Muñoz, M. C.; Real, J. A. *Coord. Chem. Rev.* **2011**, *255*, 2068. (b) Real, J. A.; Gaspar, A. B.; Muñoz, M. C. *Dalton Trans.* **2005**, 2062. (c) Hayami, S.; Kawajiri, R.; Juhász, G.; Kawahara, T.; Hashiguchi, K.; Sato, O.; Inoue, K.; Maeda, Y. *Bull. Chem. Soc. Jpn.* **2003**, *76*, 1207. (d) Kahn, O.; Martínez, C. J. *Science* **1998**, *279*, 44.

(15) (a) Ratera, I.; Veciana, J. *Chem. Soc. Rev.* **2012**, *41*, 303. (b) *Spin Crossover in Transition Metal Compounds I*; Gütlich, P., Goodwin, H. A., Eds.; Topics in Current Chemistry, Vol. 233; Springer: Berlin, 2004. (b) Gütlich, P.; Garcia, Y.; Woike, T. *Coord. Chem. Rev.* **2001**, *219*, 839. (c) Gütlich, P.; Garcia, Y.; Goodwin, H. A. *Chem. Soc. Rev.* **2000**, *29*, 419. (d) Gütlich, P.; Hauser, A.; Spiering, H. *Angew. Chem., Int. Ed. Engl.* **1994**, *33*, 2024.

(16) (a) Sagara, T.; Klassen, J.; Ganz, E. *J. Chem. Phys.* **2004**, *121*, 12543. (b) Sagara, T.; Klassen, J.; Ortony, J.; Ganz, E. *J. Chem. Phys.* **2005**, *123*, No. 014701.

(17) Lee, T. B.; Kim, D.; Jung, D. H.; Choi, S. B.; Yoon, J. H.; Kim, J.; Choi, K.; Choi, S.-H. *Catal. Today* **2007**, *120*, 330.

(18) (a) Raveendran, P.; Ikushima, Y.; Wallen, S. L. *Acc. Chem. Res.* **2005**, *38*, 478. (b) Raveendran, P.; Wallen, S. L. *J. Am. Chem. Soc.* **2002**, *124*, 12590.

(19) (a) Nelson, M. R.; Borkman, R. F. *J. Phys. Chem. A* **1998**, *102*, 7860. (b) Chakraborty, A. K.; Bischoff, K. B.; Astarita, G.; Damewood, J. R., Jr. *J. Am. Chem. Soc.* **1988**, *110*, 6947. (c) Meredith, J. C.; Johnston, K. P.; Seminario, J. M.; Kazarian, S. G.; Eckert, C. A. *J. Phys. Chem.* **1996**, *100*, 10837. (d) Jamróz, M. H.; Dobrowolski, J. C.; Borowiak, M. A. *J. Mol. Struct.* **1997**, *404*, 105.

(20) Vogiatzis, K. D.; Mavrandonakis, A.; Klopper, W.; Froudakis, G. E. *ChemPhysChem* **2009**, *10*, 374.

(21) (a) Grimme, S. *J. Comput. Chem.* **2004**, *25*, 1463. (b) Grimme, S. *J. Comput. Chem.* **2006**, *27*, 1787.

(22) (a) Getman, R. B.; Bae, Y.-S.; Wilmer, C. E.; Snurr, R. Q. *Chem. Rev.* **2012**, *112*, 703. (b) Gomez, D. A.; Combariza, A. F.; Sastre, G. *Phys. Chem. Chem. Phys.* **2009**, *11*, 9250. (c) Han, S. S.; Mendoza-Cortés, J. L.; Goddard, W. A., III. *Chem. Soc. Rev.* **2009**, *38*, 1460.

(23) (a) Kuc, A.; Heine, T.; Seifert, G.; Duarte, H. A. *Chem.—Eur. J.* **2008**, *14*, 6597. (b) Kuc, A.; Heine, T.; Seifert, G.; Duarte, H. A. *Theor. Chem. Acc.* **2008**, *120*, 543.

(24) (a) Bludský, O.; Rubeš, M.; Soldán, P.; Nachtigall, P. *J. Chem. Phys.* **2008**, *128*, No. 114102. (b) Rubeš, M.; Kysilka, J.; Nachtigall, P.; Bludský, O. *Phys. Chem. Chem. Phys.* **2010**, *12*, 6438. (c) Zukal, A.; Pulido, A.; Gil, B.; Nachtigall, P.; Bludský, O.; Rubeš, M.; Cejka, J. *Phys. Chem. Chem. Phys.* **2010**, *12*, 6413.

(25) Pianwanit, A.; Kritayakornupong, C.; Vongachariya, A.; Selphusit, N.; Ploymeerusmee, T.; Remsungnen, T.; Nuntasri, D.; Fritzsche, S.; Hannongbua, S. *Chem. Phys.* **2008**, *349*, 77.

(26) Grajciar, L.; Wiersum, A. D.; Llewellyn, P. L.; Chang, J.-S.; Nachtigall, P. *J. Phys. Chem. C* **2011**, *115*, 17925.

(27) (a) Liu, Y.; Liu, J.; Chang, M.; Zheng, C. *J. Phys. Chem. C* **2012**, *116*, 16985. (b) Amirjalayer, S.; Schmid, R. *J. Phys. Chem. C* **2012**, *116*, 15369. (c) Liu, Y.; Liu, J.; Chang, M.; Zheng, C. *Fuel* **2012**, *95*, 512. (d) Mani-Biswas, M.; Cagin, T. *Comput. Theor. Chem.* **2012**, *987*, 42. (e) Mahesh Kumar, R.; Subramanian, V. *Int. J. Hydrogen Energy* **2011**, *36*, 10737.

(28) Kanoo, P.; Reddy, S. K.; Kumari, G.; Halder, R.; Narayana, C.; Balasubramanian, S.; Maji, T. K. *Chem. Commun.* **2012**, *48*, 8487.

(29) Grimme, S. *J. Chem. Phys.* **2003**, *118*, 9095.

(30) Riley, K. E.; Pitoňák, M.; Jurečka, P.; Hobza, P. *Chem. Rev.* **2010**, *110*, 5023.

(31) Deshmukh, M. M.; Sakaki, S. *Theor. Chem. Acc.* **2011**, *130*, 475.

(32) (a) Zhao, Y.; Truhlar, D. G. *Acc. Chem. Res.* **2008**, *41*, 157. (b) Valero, R.; Costa, R.; Moreira, I. d. P. R.; Truhlar, D. G.; Illas, F. *J. Chem. Phys.* **2008**, *128*, No. 114103.

(33) Kendall, R. A.; Dunning, T. H., Jr.; Harrison, R. J. *J. Chem. Phys.* **1992**, *96*, 6796.

(34) (a) Figgen, D.; Rauhut, G.; Dolg, M.; Stoll, H. *Chem. Phys.* **2005**, *311*, 227. (b) Figgen, D.; Peterson, K. A.; Dolg, M.; Stoll, H. *J. Chem. Phys.* **2009**, *130*, No. 164108.

(35) Hay, P. J.; Wadt, W. R. *J. Chem. Phys.* **1985**, *82*, 270.

(36) Boys, S. F.; Barnardy, F. *Mol. Phys.* **1970**, *19*, 553.

(37) Frisch, M. J.; Trucks, G. W.; Schlegel, H. B.; Scuseria, G. E.; Robb, M. A.; Cheeseman, J. R.; Scalmani, G.; Barone, V.; Mennucci, B.; Petersson, G. A.; Nakatsuji, H.; Caricato, M.; Li, X.; Hratchian, H. P.; Izmaylov, A. F.; Bloino, J.; Zheng, G.; Sonnenberg, J. L.; Hada, M.; Ehara, M.; Toyota, K.; Fukuda, R.; Hasegawa, J.; Ishida, M.; Nakajima, T.; Honda, Y.; Kitao, O.; Nakai, H.; Vreven, T.; Montgomery, J. A., Jr.; Peralta, J. E.; Ogliaro, F.; Bearpark, M.; Heyd, J. J.; Brothers, E.; Kudin, K. N.; Staroverov, V. N.; Kobayashi, R.; Normand, J.; Raghavachari, K.; Rendell, A.; Burant, J. C.; Iyengar, S. S.; Tomasi, J.; Cossi, M.; Rega, N.; Millam, J. M.; Klene, M.; Knox, J. E.; Cross, J. B.; Bakken, V.; Adamo, C.; Jaramillo, J.; Gomperts, R.; Stratmann, R. E.; Yazyev, O.; Austin, A. J.; Cammi, R.; Pomelli, C.; Ochterski, J. W.; Martin, R. L.; Morokuma, K.; Zakrzewski, V. G.; Voth, G. A.; Salvador, P.; Dannenberg, J. J.; Dapprich, S.; Daniels, A. D.; Farkas, Ö.; Foresman, J. B.; Ortiz, J. V.; Cioslowski, J.; Fox, D. J. *Gaussian 09*, revision B.01; Gaussian, Inc.: Wallingford, CT, 2010.

(38) Su, P.; Li, H. *J. Chem. Phys.* **2009**, *131*, No. 014102.

(39) GAMESS (1 OCT 2010 R1): Schmidt, M. W.; Baldridge, K. K.; Boatz, J. A.; Elbert, S. T.; Gordon, M. S.; Jensen, J. H.; Koseki, S.; Matsunaga, N.; Nguyen, K. A.; Su, S.; Windus, T. L.; Dupuis, M.; Montgomery, J. A., Jr. *J. Comput. Chem.* **1993**, *14*, 1347.

(40) Ohinishi, Y.; Nakao, Y.; Sato, H.; Sakaki, S. *J. Phys. Chem. A* **2007**, *111*, 9715.

(41) For instance, upon moving from the minimum by 1 Å, the binding energy changes slightly (0.5 kcal mol^{-1}) for CO_2 but changes greatly for CS_2 (5 kcal mol^{-1}) in the ONIOM(MP2.5:M06-2X) calculation.